Elsevier Editorial System(tm) for The 37th International Conference on Metallurgical Coatings and Thin Films
Manuscript Draft

Manuscript Number: ICMCTF_2010-D-10-00073R1

Title: Thin Film Deposition and Surface Modification with Atmospheric Pressure Dielectric Barrier Discharge

Article Type: Full Length Article

Section/Category: Symposium G

Keywords: atmospheric pressure; dielectric barrier discharge; surface processing; plasma diagnostics; thin film deposition; fluorocarbon; organosilicon

Corresponding Author: Dr. Fiorenza Fanelli, Ph.D.

Corresponding Author's Institution: University of Bari Aldo Moro

First Author: Fiorenza Fanelli, Ph.D.

Order of Authors: Fiorenza Fanelli, Ph.D.

Abstract: This paper focuses on some of the most debated issues concerning the utilization of atmospheric pressure dielectric barrier discharges (DBDs) in surface processing of materials such as, for instance, the existence of different discharge regimes (filamentary and homogeneous), the influence on the discharge behaviour of feed gas additives and substrate properties (chemical composition, electrical characteristics, etc.). Crucial aspects of the DBD operation which highly differentiate this approach from the well established low pressure plasma technology will be discussed.
An overview of the state of the art in atmospheric pressure thin film deposition from fluorocarbon- or organosilicon-containing DBDs will be also provided. In particular the possibility of tailoring the chemical composition of the coatings, the etching-deposition competition and the influence of feed gas contaminants (i.e. air and H2O) in the deposition of fluoropolymers will be discussed. Recent results on the deposition of SiOxCyHz thin films from three different methyldisiloxanes (i.e. hexamethyldisiloxane, pentamethyldisiloxane and tetramethyldisiloxane) will allow to highlight the effect of the chemical structure of the organosilicon precursor and of the oxygen-to-methyldisiloxane feed ratio on the properties of the deposits. The results obtained through different diagnostic techniques of the plasma phase (i.e. optical emission spectroscopy, GC-MS analysis of the exhaust gas) and of the deposits (i.e. XPS, FT-IR, SEM, WCA) allow to highlight interesting aspects of the fluorocarbon and organosilicon plasma chemistry at atmospheric pressure.

Thin Film Deposition and Surface Modification with Atmospheric Pressure Dielectric Barrier Discharges

Fiorenza Fanelli

Dipartimento di Chimica, Università degli Studi di Bari Aldo Moro, via Orabona 4, 70126 Bari, Italy

Abstract

This paper focuses on some of the most debated issues concerning the utilization of atmospheric pressure dielectric barrier discharges (DBDs) in surface processing of materials such as, for instance, the existence of different discharge regimes (filamentary and homogeneous), the influence on the discharge behaviour of feed gas additives and substrate properties (chemical composition, electrical characteristics, etc.). Crucial aspects of the DBD operation which highly differentiate this approach from the well established low pressure plasma technology will be discussed.

An overview of the state of the art in atmospheric pressure thin film deposition from fluorocarbon- or organosilicon-containing DBDs will be also provided. *In particular the possibility of tailoring the chemical composition of the coatings, the etching-deposition competition and the influence of feed gas contaminants (i.e. air and H_2O) in the deposition of fluoropolymers will be discussed. Recent results on the deposition of $SiO_xC_yH_z$ thin films from three different methyldisiloxanes (i.e. hexamethyldisiloxane, pentamethyldisiloxane and tetramethyldisiloxane) will allow to highlight the effect of the chemical structure of the organosilicon precursor and of the oxygen-to-methyldisiloxane feed ratio on the properties of the deposits.* The results obtained through different diagnostic techniques of the plasma phase *(i.e. optical emission spectroscopy, GC-MS analysis of the exhaust gas)* and of the deposits

(i.e. XPS, FT-IR, SEM, WCA) allow to highlight interesting aspects of the fluorocarbon and organosilicon plasma chemistry at atmospheric pressure.

1. Introduction

Nowadays atmospheric pressure cold plasma technologies attract growing interest in the field of surface processing of materials since the absence of vacuum equipments is expected to result in several benefits such us the reduction of processes and reactors costs, the employment of easy-to-handle apparatuses, the easier integration into continuous production lines. Among the different electrical discharges which allow to establish non-thermal plasma conditions at atmospheric pressure, dielectric barrier discharges (DBDs) can be considered one of the most popular approaches [1-3]; the strong thermodynamic non-equilibrium conditions and the simple design are the main features of DBDs which favoured the expansion of their application also to surface modification [1-3]. DBDs generation in fact simply requires the presence of at least one dielectric layer located in the current path between the metal electrodes in order to prevent arc transition, and the utilization of an alternated current (AC) high voltage (HV) power supply in the typical frequency range 0.5 – 500 kHz [1-3].

Recently research efforts have been directed to evaluate if atmospheric pressure DBDs can be competitive with respect to the well established low pressure plasma processes also in some specific applications which require feed gases different than air (e.g. polymer treatment, thin films deposition, plasma-etching or plasma-cleaning, etc.).

Several open questions are debated; some of the hot topics are for instance the different discharge regimes, the effect on the discharge behaviour of feed gas additives and impurities, the influence of substrate properties (e.g. chemical composition, electrical characteristics, shape), etc..

These and other aspects are examined in this contribution that first outlines some peculiarities of DBD-based processes which highly differentiate this approach from the low pressure operation.

Some recent results on fluoropolymer deposition, concerning the tuning of the chemical composition of the deposits, the etching-deposition competition and the influence of feed gas contaminants are reported along with the latest studies on the PE-CVD (plasma-enhanced chemical vapour deposition) in DBDs fed with different methyldisiloxanes. The utilization of different diagnostic techniques of the *gas* phase and of the deposits contributed to the identification of the main reaction pathways and to the correlation of the plasma chemistry with the coatings properties. Interesting results were obtained with the optical emission spectroscopy (OES) investigation of the discharge and with the quali-quantitative determination of stable by-products contained in the DBD exhaust performed by gaschromatography coupled to mass spectrometry (GC-MS).

2. Atmospheric pressure DBDs: key-issues in surface processing of materials

2.1 Discharge regimes

The most important peculiarity of atmospheric pressure dielectric barrier discharges is their possible operation under completely different discharge regimes *[1-4]*; this aspect highly differentiates DBDs from low pressure glow discharges and often complicates their employment in surface processing of materials.

DBDs generally exhibit two major discharge modes, namely the filamentary regime and the homogeneous or diffuse regime. It is well-known that in most cases DBDs operate in the filamentary regime (i.e. filamentary dielectric barrier discharges, FDBD) characterized by many short-living (~ 10 ns time duration), narrow (~ 100 μm diameter) microdischarges (MDs) evenly and randomly distributed in time and space in the discharge gap over the dielectric surface [1-3]. The statistical distribution of MDs should confer to the FDBD an overall uniform appearance, however, as highlighted by Fridman et al. [2,3], at the usual

operation frequencies they repeatedly form at the same locations as the polarity of the applied voltage changes and hence can be macroscopically observed with the naked eye as bright spatially localized filaments.

Under particular experimental conditions homogeneous microdischarge-free regimes can be also obtained. *As reported by several authors, two kinds of homogeneous discharge generally exist: the glow-like discharges and the Townsend-like discharges [5,6]. Homogeneous DBDs fed by noble gases (e.g. helium [4-9]) are qualified as glow-like discharges (atmospheric pressure glow discharges, APGD, or glow dielectric barrier discharges, GDBD) characterized by the formation in the region near to the cathode of a positive space charge which produces a strong electric field variation known as cathode voltage fall. In APGDs four specific regions typical of a low pressure glow discharge [10] were identified by Massines et al [5]: (i) a strong cathode fall, (ii) a negative glow positioned as a bright sheath at the end of the cathode voltage fall, (iii) a Faraday dark space, characterized by a small space charge and luminosity and (iv) a positive column with a constant field. Typical APGD current densities range between 10 and 100 mA·cm^{-2}, while the maximum electron density is about 10^{10} - 10^{11} cm^{-3} [5,6]. The typical behaviour of Townsend-like discharges (atmospheric pressure Townsend discharges, APTD, or Townsend dielectric barrier discharges, TDBD) is exhibited by the low-current homogeneous discharges obtained in molecular gases such as N_2 [5,6,11]. In this case the ionization level is so low that the electric field is quasi-uniform over the discharge gap, and the cathode fall does not develop. As demonstrated by Massines et al. [5,6], in fact, in an APTD even when the discharge current is maximum the ion density is not high enough to localize the electric field in a cathode fall; the electron density grows from cathode to anode producing a higher density of excited species and hence discharge light localization at the anode. In the case of an APTD both the current density and the maximum electron density are lower than for an APGD and are in the range ~ 0.1 – 10 mA·cm^{-2} and ~ 10^{7} – 10^{8} cm^{-3}, respectively [5,6].*

In order to give an accurate picture of the multiplicity of DBD regimes it is also worth to mention the existence of notable exceptions and deviations from the normal filamentary or homogeneous modes, such as, for instance, the formation of static or time-dependent dynamic patterned regimes [*4*,12-*14*] that can be due to regularly arranged clusters of both glow regions [12] or filaments [13,*14*].

Different diagnostics tools have been employed to assess and monitor the DBD regime, e.g. the discharge current signal acquisition [5,6], the total light emission measurement [12,15], the high-speed imaging [5,6,12,16-18]. Modelling and theoretical studies contributed to explain the experimental results and to gain insights into the breakdown mechanisms, the plasma physics, the role of different species (e.g. electrons, ions, metastables, etc.) and several electro-technical issues [5,6,11,12,16-24]. Despite the great deal of work produced, an unanimous understanding and control of the homogeneous regimes has not been achieved so far [6]. Several studies demonstrated, in fact, that the operational window and stability of these regimes is strictly related to both the experimental conditions and the mechanical and electrical characteristics of the apparatuses, such as the feed mixture (i.e. main gas, nature and concentration of feed gas additives), the electrode configuration, the dielectric nature and permittivity, the applied voltage, *the* excitation frequency, the power supply and the presence of additional elements in the external electrical circuit (e.g. an impedance matching unit [20,21] or a LC circuit for electronic stabilization [22-24]).

The feed gas plays a decisive role: it seems, in fact, relatively easy to obtain homogeneous regimes in helium and nitrogen, while contrasting results are reported for other gases such as air and argon. Several authors demonstrated, for instance, that a homogeneous regime (the glow regime) can not be obtained in pure argon unless low concentration of acetone [25] or ammonia [6] are added. However other authors reported the possibility of obtaining *homogeneous* regimes in several pure gases, such as argon, air, oxygen, carbon dioxide, etc. [20,22-24,26], and *in various feed gas mixtures as it will be shown in the next section*.

2.2 Influence of feed gas additives

Studies devoted to the investigation of the different discharge regimes and to the transition between them have showed that homogeneous discharges (e.g. He glow and N_2 Townsend DBDs) are extremely susceptible to feed gas additives (often referred to as "impurities") which, if present in the reactor above certain concentration levels, may cause the transition from a *homogeneous* to a filamentary regime. For instance, Miralaï et al. [15] demonstrated that 500 ppm of O_2 or 2500 ppm of H_2 in nitrogen can completely change the discharge regime from homogeneous to filamentary; Brandenburg et al. [27] showed that an air content higher than 800 ppm in He is responsible for both the transition from a *homogeneous* to a filamentary mode and the increase of the gas breakdown voltage.

The influence of feed gas additives on DBD operation has been accurately evaluated in the optimization of PE-CVD processes which requires the addition of at least one compound (i.e. the film precursor) to the main gas. In the case of the SiO_2-like films deposition from hexamethyldisiloxane (HMDSO), Enache et.[28] al found out that with N_2-HMDSO-N_2O mixtures the Townsend regime can be successfully obtained at HMDSO concentrations lower than 20 ppm, while the N_2O content can be as high as few hundreds of ppm. In the case of fluoropolymers deposition in helium-fluorocarbon fed DBDs Fanelli et al. [29] showed that the typical features of a glow discharge can be obtained at fluorocarbon concentrations lower than 0.01% and 0.025% for hexafluoropropene (C_3F_6) and octafluoropropane (C_3F_8), respectively. However Aldea et al., by using suitable electronic stabilization of the fast current variations to prevent glow to arc transition, dynamic matching and particular discharge assembly, demonstrated that the APGD can be successfully achieved for a wide range of plasma parameters and feed gas mixtures at additive gas concentrations as high as 50% [*16,17*,22-24,30,31]. These results indicate that it is possible to enlarge the homogeneous discharge operational window and that it is possible to obtain the *homogeneous* regime under experimental conditions very close to the practical applications. In ref. [*17*,31] the uniform large area deposition of SiO_2-like layers was, in fact, performed with a *homogeneous* DBDs

fed with an Ar-N_2 main flow, O_2 (about 15000 ppm) and HMDSO (80 ppm) as reactive species, *while in ref. [18] the homogeneous DBD was operated with air as main flow in mixture with Ar-HMDSO (0.1 sccm-0.4 g·h^{-1}). The formation and temporal evolution of the homogeneous DBD at atmospheric pressure in these PE-CVD processes was studied by fast discharge imaging and electrical diagnostics. In particular in. Ar-N_2-O_2-HMDSO mixtures [17], it was found that the discharge gradually experiences the following three phases: (i) homogeneous low-current Townsend-like mode in which the discharge uniformly occupies the whole electrode surface and light emission comes from the region near to the instantaneous anode; (ii) local Townsend to glow transition in which, at a certain moment, at one or several locations in the gap glow-like current spots form; this transition to the glow mode is accompanied by an increase of charged particle densities, discharge current and light emission intensity; (iii) expanding high current density glow-like mode in which a lateral discharge expansion occurs, i.e. the bright current spots move along the electrodes providing uniform treatment of the whole substrate. This study allowed to reveal in a glow-like DBD fed with helium-free mixtures another important feature previously observed only in helium fed APGDs [8,9]), namely the fact that atmospheric pressure high current glow-like discharges can occupy only a part of the of the electrode as low pressure subnormal and normal glow discharges [10].*

Besides the discharge regime, also the overall stability of the DBD *needs* a tight monitoring. Under fixed conditions of excitation voltage and frequency, additives concentrations above a certain threshold value can result in the contraction of the discharge volume. Fig. 1 shows the photographs of an Ar-N_2 fed DBD generated in a parallel plate electrode reactor [32]. If the N_2 concentration exceeds the threshold level of 0.3% the discharge is not distributed over the entire electrode surface and starts to contract. This phenomenon can be appreciated as a shrinking of the discharge that, as evident in Fig. 1, starts from the electrode edges and generally, for a lateral feed gas injection, from the gas outlet. It is worth to mention that above the N_2 threshold limit of 0.3%, it is possible to restore a stable discharge over the entire electrode surface by simply increasing the applied voltage. *This evidence clearly shows that*

N_2 addition increases the applied voltage required to sustain the discharge [27], likely as a consequence the discharge energy dissipation due to the translational, rotational and vibrational excitation of the molecular gas (N_2) added to the noble gas (Ar). It seems also reasonable that with increasing the gas residence time into the discharge gap these energy dissipation mechanisms become more and more important and, hence, it could be most probable that the condition of discharge quenching is reached near to the gas outlet.

2.3 The substrate

Due to the atmospheric pressure operation, DBD ignition requires small gas gaps [1-3] and, in fact, parallel plate electrode systems, widely employed in surface treatment, are commonly characterized by discharge gaps ranging between 1 and 5 mm. This architectural limit can have several consequences on the choice of the substrates to be treated; parallel plate apparatuses can be used only for the surface modification of flat substrates. The treatment of three-dimensional substrates generally requires remote discharge operation, in which they are placed downstream of the discharge zone, and/or the utilization of specific DBD sources. Discharges that are not spatially bound or confined by electrodes can be produced with DBD torches or jets *[33-35];* due to the high feed flow rate (several slm), in fact, the discharge is launched outside the zone where it is generated, forming a plasma plume that *is in contact with* the substrate surface.

As a consequence of the small discharge gap of DBDs, the ratio between the discharge area and volume is quite high and, therefore, the micro- and macroroughness of the substrate to be treated, the presence of impurities on the substrate surface or in its pores can deeply affect the processes.

Naudé et al. [36] investigated also the influence of the substrate surface conductivity on the stability of a glow DBD. They illustrated that a non-insulating surface (e.g. a silicon wafer) in contact with a glow discharge induces the formation of microdischarges. Using a continuous

sinusoidal excitation voltage, they observed that microdischarges only occur during the positive half-cycle of the excitation voltage, when the non-insulating surface is at the cathode side and that their duration is very long (few μs). As long as the wafer is not changed microdischarges are generated always at the same place producing a significant surface damage. This phenomenon was explained considering that surface charges accumulate on insulating materials at the microdischarge position inducing a significant local decrease of the applied voltage which promotes the MD extinction. However, if the surface conductivity is high, as in the case of a Si wafer, the charge deposited by the microdischarge spreads all over the substrate surface and the local variation of the potential is too small to stop the microdischarge.

A similar phenomenon can be also observed in filamentary discharges. As evident in Fig. 2, if a Si substrate is positioned in a parallel plate filamentary DBD, in this case fed by Ar-CF_4 mixtures *(Ar-0.6% CF_4, 10 kHz, 7.6 kV_{p-p}, 2 mm gas gap),* intense filaments visible with the *naked eye (Fig. 2a)* form repeatedly at the same location inducing severe substrate damage in the form of craters *as evident from the optical microscope image in Fig. 2b corresponding to a treatment duration of 10 min. The higher the treatment time, the more evident the substrate damage*. This drawback can be overcome by a careful choice of the experimental conditions, by moving the sample into the discharge area, or by using pulsed power supplies that can improve the statistical distribution of microdischarges over the surfaces.

3. Atmospheric pressure PE-CVD of fluorocarbon thin films

Recently, many investigations on the PE-CVD of fluorocarbon thin films in atmospheric pressure DBDs have been published. One of the first investigations was reported by Yokoyama et al. [37] which used tetrafluoroethylene (C_2F_4) in mixture with high flow rates of

helium in order to generate an APGD. Coatings with a F/C ratio in the range 1.4-1.7 were obtained with deposition rates as high as 2 $\mu m \cdot h^{-1}$. This fundamental study was followed by applicative papers presenting innovative processes and apparatuses for the deposition of fluoropolymers on powders [38] and on the inner surface of polymeric tubes [39].

Vinogradov et al. [40,41] investigated the deposition of fluorocarbon films in filamentary DBDs fed with different fluorocarbons, e.g. CF_4, C_2F_6, $C_2H_2F_4$, C_3F_8, C_3HF_7 and c-C_4F_8, in mixture with Ar; an in situ investigation of the plasma phase was performed by means of UV absorption spectroscopy, Fourier Transform Infrared (FT-IR) absorption spectroscopy, and optical emission spectroscopy.

In the last few years the possibility of tailoring the chemical composition (i.e. the F/C ratio) and the crosslinking of the deposited thin films at atmospheric pressure has been demonstrated. As widely reported for low pressure plasmas [42,43], it was shown that by simply varying the H_2 concentration in He-C_3F_8-H_2 fed glow DBDs [29,44] it is possible to tune the F/C ratio of the coating from 1.5 to 0.6, and, hence, its wettability.

The investigation of He-C_3F_8-H_2 fed GDBDs, by means of OES allowed to detect the features due to He, F and H atoms as well as to CF_2 ($A^1 B_1 – X^1 A_1$ system), CF_2^+ (continuum centred at about 290 nm), and CH ($A^2\Delta$- $X^2\Pi$ system) [29,44] as reported for low pressure plasmas [42,43]. Even though at atmospheric pressure the actinometric approach can not be utilized to estimate the relative concentration of emitting species in the ground state, the OES results have been correlated to the properties of the deposited film. In fact, as shown in Fig. 3 the water contact angle (WCA) of the coatings decreases with increasing the CH/CF_2 emission intensity ratio, which in turn increases as a function of the H_2 content in the feed.

The competition between the deposition and the etching of fluorocarbon thin films in atmospheric pressure DBDs was also investigated with Ar–CF_4–H_2 and Ar–CF_4–O_2 mixtures [32]. This is an interesting topic debated in the 80's by the scientific community involved in

the study of dry etching/polymerization processes in fluorine-containing low pressure plasmas [42,43,45,46]. The results indicate that both processes occur contemporaneously at high pressure, there is in fact a competition very similar to that observed in low pressure plasmas. The most important difference with respect to the low pressure operation is the negligible effect of ion bombardment at atmospheric pressure due to the high collision probability which limits the ion energy.

In Fig. 4a it is shown that H_2 addition to CF_4 promotes thin films deposition; no deposition is obtained below 10% H_2 and a deposition rate maximum of about 18 nm·min^{-1} is registered at 20% H_2. In order to study the dry etching of fluoropolymers, a film deposited in Ar–CF_4–20% H_2 was exposed in Ar–CF_4–O_2 fed DBDs (Fig. 4b). *To detect the etch rate of plasma-deposited fluoropolymers thickness measurements were performed before and after plasma etching in Ar–CF_4–O_2 [25].* Without oxygen, an etch rate of 7 nm min^{-1} is detected indicating that, as in low pressure plasmas [42,43,45], fluoropolymers can be etched by fluorine atoms. Oxygen addition enhances the etching and without CF_4 (i.e. with Ar–O_2 fed FDBDs) an etch rate as high as to 62 nm min^{-1} is measured. Since at atmospheric pressure the effect of ion bombardment is negligible, it is possible to conclude that the plasma-deposited fluoropolymers can be etched by the fluorine atoms through pure chemical reactions (i.e. pure chemical etching). As a consequence anytime a DBD is fed with fluorocarbon mixtures the fluorocarbon radicals are responsible of the film growth (i.e. plasma polymerization) and the fluorine atoms act as etchants of the growing film (i.e. dry etching): this is the deposition-etching competition.

The optical emission spectra in the 190 – 380 nm wavelength range of Ar-CF_4-O_2 filamentary DBDs are reported in Fig. 5. The spectra are dominated by an intense narrow emission at 193 nm and a broad continuum centred at 290 nm ascribed to ArF and Ar_2F excimers, respectively [47]. Without oxygen, several emission features of CF and CF_2 are overimposed to the continuum emission centred at 290 nm, which also includes the broad emission of CF_2^+. O_2

addition to the feed reduces the emissions of fluorocarbon fragments while the emissions of excimers remain extremely intense. Surprisingly any signal from F atoms was not detected under the experimental conditions investigated, even though the fluoropolymer etching measured in Ar-CF_4 DBDs demonstrates that reactive fluorine is present in the discharge. It is important to report that if the emission of Ar-O_2 DBD is collected with the dielectric surfaces coated by a fluoropolymers deposited in previous experiments, intense emissions from ArF and Ar_2F are detected due to the etching of the fluoropolymer and the consequent release in the DBD gap of F atoms and fluorocarbon fragments; these emissions disappear when the fluoropolymer is completely removed from the surfaces exposed to the discharge.

Excimers formation, which generally requires three-body collisions, is favoured by the high pressure operation of DBDs [1]. As reported for electron-beam excited Ar-F_2 mixtures and excimer laser [48,49], two main reaction pathways can lead to the formation of ArF excimer: an ionic channel, i.e. a three-body reaction in which Ar^- and F^- ions recombine in the presence of an argon atom, and a neutral channel, i.e. a harpoon reaction between an excited argon atom and F_2. Once formed, ArF excimer can generate Ar_2F from a third-body reaction with two Ar atoms [48,49].

Even though very interesting results have been published on the atmospheric pressure PE-CVD of fluorocarbon thin films by dielectric barrier discharges (DBDs), the utilization of atmospheric pressure plasma technologies in this field is still a challenge.

Research efforts should be devoted to evaluate if DBDs can actually be advantageous compared to low-pressure plasmas for fluoropolymer deposition. For this purpose, besides the fundamental investigation of the PE-CVD in DBDs fed with different fluorocarbons, it is also important to gain insights into the influence of contaminants such as air and water vapour on the deposition process. The presence of these impurities in the atmospheric pressure reactors

could have, in fact, a serious detrimental effect on the overall deposition process because it could result in a change of the discharge regime, in a variation of the polymer composition, in oxygen and nitrogen uptake, as well as in deposition rate variation. On the other hand, the knowledge of the highest level of contamination, compatible with an acceptable process performance, and consequently, the possibility of depositing fluorocarbon films with the desired properties in contaminated environments could allow reduction of the cost of processes and reactors.

For these reasons, the influence of contaminants on the deposition process was investigated in an airtight system by adding controlled amounts of air and water vapour to the feed gas mixtures, in order to simulate the contamination [50]. A FDBD fed with argon and 0.2% of hexafluoropropene was selected for this study. The presence of a double bond in C_3F_6 accounts for its high polymerizing capability, both in low pressure [51] and atmospheric pressure plasmas [29,44,50]. Without contaminants, the average power dissipated by the plasma is 22 W, the deposition rate is 56 $nm \cdot min^{-1}$ and the deposit is characterized by a XPS (X-ray Photoelectron Spectroscopy) F/C ratio of 1.7 and a static WCA of 115° [50]. Since the most important features of the XPS C1s signal are the CF_3 and CF_2 components, the fluoropolymer is characterized by a low branching and cross-linking.

Contaminants addition results in a decrease in discharge power, and at water and air molar concentrations of 0.05 and 0.1%, respectively (corresponding to Air-to-C_3F_6 and Air-to-H_2O molar ratios of 0.25 and 0.5, respectively) the discharge is not distributed over the entire electrode surface and starts to contract.

As it can be appreciated in Fig. 6, air and water vapour addition decreases the deposition rate but does not significantly affect the XPS F/C ratio of the coating, as well as the O and N uptakes which were always lower than 1%. When the 0.1% of air is added to the feed, the deposition rate decreases 30 $nm \cdot min^{-1}$, while for a water vapour concentration of 0.05%, the deposition rate is reduced to 26 $nm \cdot min^{-1}$. Contaminants addition does not affect the WCA

while it induces a clear variation of film morphology due to the appearance of a slight roughness, more evident for air [50].

These encouraging results indicate that process performance remains acceptable, in terms of deposition rate and fluoropolymer composition, even though further investigations are needed. For example it is necessary to evaluate the production of toxic compounds, such as flurophosgene (CF_2O), due to the presence of contaminants.

4. Thin film deposition from organosilicon-containing DBDs

The utilization of organosilicon compounds, such as hexamethyldisiloxane and tetraethoxysilane (TEOS) in mixture with oxidants (i.e. O_2 and N_2O) and/or noble gases has been and is still widely investigated in low pressure PE-CVD processes [52-56]. The versatility of these reactive plasmas due to the tunability of the chemical composition of the deposits from silicone-like to SiO_2-like has been clearly shown. Large-scale applications in several technological fields such us microelectronics, flexible packaging, corrosion protection, biomedical application, optics, etc. have been found or are presently under evaluation.

The interest of the academic community has been recently expanded to atmospheric pressure glow discharges fed with organosilicon containing mixtures. DBDs, both in filamentary and glow regime, have been proposed for PE-CVD on several substrates (e.g. polymers and metals) for different applications [57-67].

Massines et al., working with Atmospheric Pressure Townsend Discharges fed with N_2-HMDSO-N_2O mixtures, varied the chemical composition of the deposits by changing the N_2O-to-HMDSO ratio [28,60,61]; inorganic and dense SiO_2-like thin films with negligible carbon and nitrogen incorporation but detectable Si-OH groups were obtained at high ratios.

These authors also investigated the influence of the feed flow rate and injection design on film homogeneity [61].

The deposition of high quality SiO_2-like layers on large area polymeric substrates in a roll-to-roll reactor was performed by means of homogeneous DBDs fed with Ar-N_2-O_2-HMDSO [17,30,31] and Air-HMDSO [18] mixtures. It was also demonstrated that the formation of powders, which reduces the quality of the deposit, can be avoided by using a pulsed power supply and adequate gas residence times in the discharge zone. The use of cycle periods (pulse-on time plus pulse-off time) close to the gas residence time limits the formation of dust in the discharge [30].

Besides these studies, an increasing number of publications focused also on the aerosol-assisted atmospheric pressure plasma deposition in which the liquid organosilicon compound is introduced in the DBD as a finely dispersed aerosol. Several monomers have been used (e.g. octamethylcyclotetrasiloxane, polydimethylsiloxane, tetramethyldisiloxane, tetraethoxysilane, etc.) and, without oxygen addition, the deposited films are characterized by high retention of the monomer structure [64,65].

As evident also from the above overview, most published studies deal mainly with the performances of the PE-CVD process in terms of deposition rates, deposit homogeneity, chemical composition and properties, few works focus on the deposition mechanism. For this reason the research should be addressed to detect the film precursors, to identify the main reaction pathways (both homogeneous and heterogeneous processes) and to clarify the plasma-surface interaction. These studies, which would probably lead to an easier reactor and process scale up, generally require the utilization of different diagnostic techniques. Among the few published studies concerning the chemistry of organosilicon fed plasma it is worth mentioning those of Vinogradov et al. which with FT-IRAS and OES investigated DBDs fed with Ar-HMDSO-O_2 and He-HMDSO-O_2 [66].

A powerful indirect diagnostic technique of the plasma phase which can provide useful information on the plasma chemistry is the gaschromatography with mass spectrometric detection. As widely demonstrated for low pressure plasma [52,53,56], as soon as a suitable exhaust sampling procedure is optimized, GC-MS can improve the understanding of the plasma chemistry, since it allows the evaluation of the precursor reactivity, the qualitative and eventually quantitative determination of stable by-products formed after plasma activation. The first work concerning the utilization of GC-MS for the investigation of organosilicon-containing atmospheric pressure DBDs was published in 2001 by Sonnenfeld et al. [58]. This diagnostic technique was later coupled to the characterization of deposited thin films with the aim of contributing to the understanding of thin film deposition in atmospheric pressure plasmas [67].

A parallel plate DBD fed by argon in mixture with oxygen and different methyldisiloxanes i.e. hexamethyldisiloxane, pentamethyldisiloxane (PMDSO) and tetramethyldisiloxane (TMDSO) has been recently utilized to investigate the influence of the chemical structure of the organosilicon precursor and of the oxygen-to-monomer feed ratio on the properties of the deposited coatings and on the composition of the exhaust gas. Whatever the organosilicon precursor, it is possible to tune the chemical composition of the deposits from silicone-like to SiO_2-like by increasing the O_2-to-monomer feed ratio. As shown by the FT-IR spectra of the deposits reported in Fig. 7, without O_2 addition to the feed, the chemical composition of the plasma deposited thin film reflects that of the monomer. The IR absorption of carbon-containing groups (i.e. CH_x and $Si(CH_3)_x$) [52,55,60,67] increases with the number of methyl groups contained in the organosilicon precursor (i.e. HMDSO > PMDSO > TMDSO), and the Si-H absorption at about 2125 cm^{-1} [52,55,60,67] with the number of Si-H bonds (i.e. TMDSO > PMDSO > HMDSO). Oxygen addition to the feed promotes the steep reduction of the carbon-containing moiety absorptions which, at a O_2-to-monomer ratio of 12, completely disappear in the case of TMDSO while they are still visible for the other two monomers, that

require a higher stoichiometric amount of O_2 for a complete oxidation. The increase of the O_2 content in the feed also results in the appearance of silanol absorptions and in the shift of the intense SiOSi asymmetric stretching band from 1040 cm^{-1} to higher wavenumbers [52,55,60,67].

The GC-MS investigation of the exhaust gas allowed to assess the percent of unreacted monomer and therefore the monomer depletion (i.e. the amount of the organosilicon precursor transformed by the plasma). Fig. 8 shows that the depletion is not enhanced by the addition of oxygen to the feed gas. In the case of HMDSO a depletion reduction from 76 to 50% is registered when the O_2-to-monomer ratio in the feed is increased from 0 to 40. For PMDSO and TMDSO the variation of monomer depletion with oxygen addition is negligible.

The qualitative analysis of the exhaust shows the formation of many different linear and cyclic compounds containing up to five silicon atoms [56,67]. Among them some silanes (e.g. trimethylsilane and tetramethylsilane) are identified, indicating the dissociation of the Si-O bond contained in the monomer. Linear and cyclic methyldisiloxanes with the general formula $SiMe_3$-$(Me_2SiO)_n$-$SiMe_3$ (n = 1–4) and $(Me_2SiO)_n$ (n = 3–4) are also formed for the occurrence of oligomerization, ring formation and expansion reactions; some of these species present –MeHSiO– units (*e.g. heptamenthyltrisiloxanes*). Finally the presence of silanol containing compounds (e.g. trimethylsilanol and hydroxypentamethyldisiloxane) is revealed.

The number and concentration of oligomers containing from 3 to 5 silicon atoms decrease with decreasing the number of methyl groups in the three precursor investigated. As an example tetrasiloxanes and pentasiloxanes are observed only with HMDSO, while trisiloxanes (e.g. octamethyltrisiloxane, 1,1,1,3,5,5,5-heptamethyltrisiloxane and 1,1,1,3,3,5,5-heptamethyltrisiloxane) are detected with HMDSO and PMDSO.

Oxygen addition results in the steep decrease of the concentration of most silanes and siloxanes below the quantification limit likely for oxidation reactions. This trend is well correlated with the variation of the chemical composition of the deposited film provoked by

oxygen addition to the feed. A different behaviour is observed for silanols. For instance, Fig. 9 shows that the concentration of hydroxypentamethyldisiloxane decreases as a function of the O_2-to-HMDSO ratio in the feed, but it is never below the detection limit; while for PMDSO the flow rate of hydroxypentamethyldisiloxane increases with O_2 concentration. This different trend which could be a consequence of reactions involving the Si-H bond clearly indicates that the content of silanol *groups* in the deposit is not correlated with the silanols content in the exhaust.

5. Conclusions

The confident utilization of atmospheric pressure DBDs in surface treatment of materials strictly requires the knowledge of the most important aspect of their operation. The main feature of DBDs is their possible existence in different discharge regimes characterized by operational windows dependent on the experimental conditions and reactor mechanical and electrical characteristics. The chemical composition of the feed gas plays a crucial role in the DBD operation since it can influence not only the discharge regime but also the discharge stability over the electrode area. The plasma apparatuses and process conditions have also to be adapted to the substrate considering its chemical composition, electrical characteristics and shape.

Concerning the PE-CVD in fluorocarbon containing DBDs, it was demonstrated that it *is* possible to tune the chemical composition and properties of the deposits and that, as observed in low pressure plasmas, there is a deposition-etching competition. If C_3F_6 is used as fluorocarbon precursor, the process performance remains acceptable in terms of deposition rate and chemical composition also at relatively high contamination (air and water vapour) concentration in the reactor.

The PE-CVD in FDBDs fed by argon in mixture with oxygen and different methyldisiloxanes highlighted that it is possible to tune the chemical composition of the deposits from silicone-like to SiO_2-like by increasing the O_2-to-monomer feed ratio. Oxygen addition to the feed promotes the steep reduction of the carbon-containing moiety of the deposits, however this decrease is less evident with increasing the number of methyl groups in the organosilicon molecule. The GC-MS investigation of the exhaust gas allowed to assess the monomer depletion, to identify several by-product (e.g. silanes, siloxanes, silanols) formed by plasma activation. As expected, O_2 addition results in the steep decrease of the concentration of most silanes and siloxanes below the quantification limit likely due to oxidation reactions. A different behaviour is observed for silanols, which is not correlated with the content of silanol groups in the deposits.

Acknowledgements

The author would like to express her deepest gratitude to Prof. Riccardo d'Agostino and Prof. Francesco Fracassi (University of Bari Aldo Moro, Bari, Italy) for the guidance and the many inspiring and valuable discussions. The author gratefully acknowledges also Dr. Sara Lovascio and Mr. Giovanni Di Renzo for the scientific collaboration, Mr. Savino Cosmai for the technical assistance and Mrs. Roberta Giordano for the photographs of the DBD. The financial support of Regione Puglia (CIP: PE_083) is acknowledged.

References

1. U. Kogelschatz, Plasma Chem. Plasma Process., 23 (2003) 1.
2. A. Fridman, A. Chirokov and A. Gutsol, J. Phys. D. Appl. Phys., 38 (2005) R1.
3. A. Fridman, Plasma Chemistry, Cambridge University Press, New York, 2008.
4. *U. Kogelschatz, IEEE Trans. Plasma Sci., 30 (2002) 1400.*

5. F. Massines, P. Ségur, N. Gherardi, C. Khamphan and A. Ricard, Surf. Coat. Technol., 174-175 (2003) 8.

6. F. Massines, N. Gherardi, N. Naudé and P. Ségur, Eur. Phys. J. Appl. Phys. 47 (2009) 22805.

7. S. Kanazawa, M. Kogoma, T. Moriwaki and S. Okazaki, J. Phys. D: Appl. Phys. 21 (1988) 838.

8. L. Mangolini, K. Orlov, U. Kortshagen, J. Heberlein and U. Kogelschatz, Appl. Phys. Lett., 80 (2002) 1722.

9. H. Luo, Z. Liang, B. Lv, X. Wang, Z. Guan and L. Wang, Appl. Phys. Lett., 91 (2007) 231504.

10. Y. P. Raizer, Gas Discharge Physics, Springer, Berling, 1991.

11. Y. B. Golubovskii, V. A. Maiorov, J. Behnke and J. F. Behnke, J. Phys. D: Appl. Phys., 35(2002) 751.

12. I. Radu, R. Bartnikas, G. Czeremuszkin and M. R. Wertheimer, IEEE Trans. Plasma Sci., 31 (2003) 411.

13. E. Ammelt, D. Schweng and H.-G. Purwins, Phys. Lett., 179 (1993) 348.

14. L. Stollenwerk, Sh. Amiranashvili, J.-P. Boeuf, and H.-G. Purwins, Phys. Rev. Lett., 96 (2006) 255001.

15. S. F. Miralaı, E. Monette, R. Bartnikas, G. Czeremuszkin, M. Latrèche and M. R. Wertheimer, Plasmas Polym., 5 (2000) 63.

16. S. A. Starostin, M. A. M. ElSabbagh, E. Aldea, H. de Vries, M. Creatore and M.C.M. van de Sanden, IEEE Trans. Plasma Sci., 36 (2008) 968.

17. S. A. Starostin, P. A. Premkumar, M. Creatore, E. M. van Veldhuizen, H. de Vries, R. M. J. Paffen and M. C. M. Van de Sanden, Plasma Sources Sci. Technol, 18 (2009) 045021.

18. S. A. Starostin, P. A. Premkumar, M. Creatore, H. de Vries, R. M. J. Paffen and M. C. M. Van de Sanden, Appl. Phys. Lett., 96 (2010) 061502.

19. N. Naudé, J-P Cambronne, N. Gherardi and F. Massines, J. Phys. D: Appl. Phys., 38 (2005) 530.

20. J. R. Roth, P. Tsai, C. Liu, M. Laroussi and P. D. Spence, U.S. Patent No. 5414324, 9 May 1995.

21. Z. Chen, IEEE Trans. Plasma Sci., 30 (2002) 1922.

22. E. Aldea, P. Peeters, H. de Vries and M.C.M van de Sanden, Surf. Coat. Technol., 200 (2005) 46.

23. H. W. de Vries, F. Mori, E. Aldea and M. C. M. van de Sanden, U.S. Patent No. 6774569, 10 Aug. 2004.

24. H. W. de Vries, Y. Kamiyama, J. B. Bouwstra, M. C. M. van de Sanden, E. Aldea and P. Peeters, Eur. Patent No. 1626613 A1, 15 Feb. 2006.

25. S. Okazaki, M. Kogoma, M. Uehara and Y. Kimura, J. Phys. D: Appl. Phys. 26 (1993) 889.

26. J. R. Roth, J. Rahel, X. Dai and D. M. Sherman, J. Phys. D: Appl. Phys., 38 (2005) 555.

27. R. *Brandenburg*, Z. Navratil, J. Jasly, P. Stahel, D. Trunec and H.-E- Wagner, J. Phys. D: Appl. Phys., 42 (2009) 085208.

28. I. Enache, H. Caquineau, N. Gherardi, T. Paulmier, L. Maechler and F. Massines, Plasma Processes Polym., 4 (2007) 806.

29. F. Fanelli, R. d'Agostino and F. Fracassi, Plasma Process. Polym., 4 (2007) 797.

30. H. W. de Vries, E. Aldea, S. A. Starostin, M. Creatore and M. C. M. van de Sanden, Eur. Patent No. 2024533 A1, 18 Feb. 2009.

31. P. A. Premkumar, S. A. Starostin, H. de Vries, R. M. J. Paffen, M. Creatore, T. J. Eijkemans, P.M. Koenraad and M. C. M. van de Sanden, Plasma Process. Polym., 6 (2009) 693.

32. F. Fanelli, F. Fracassi and R. d'Agostino, Surf. Coat. Technol., 204 (2010) 1779.

33. M. Laroussi and T. Akan, Plasma Process. Polym., 4 (2007) 777.

34. M. Laroussi, in R. Hippler, H. Kersten, M. Schmidt and K. H. Schoenbach (eds.), Low Temperature Plasmas. Fundamentals, Technologies and Techniques, Wiley-VCH, Berlin, 2008, vol. 2, p. 821.

35. E. Stoffels, in R. Hippler, H. Kersten, M. Schmidt and K. H. Schoenbach (eds.), Low Temperature Plasmas. Fundamentals, Technologies and Techniques, Wiley-VCH, Berlin, 2008,vol. 2, p. 837.

36. N. Naudé and F. Massines, IEEE Trans. Plasma Sci., 36 (2008) 1322.

37. T. Yokoyama, M. Kogoma, S. Kanazawa, T. Moriwaki and S. Okazaki, J. Phys. D: Appl. Phys., 23 (1990) 374.

38. Y. Sawada and M. Kogoma, Powder Technol., 90 (1997) 245.

39. Y. Babukutty, R. Prat, K. Endo, M. Kogoma, S. Okasaki and M. Kodama, Langmuir, 15 (1999) 7055.

40. I. P. Vinogradov, A. Dinkelmann and A. Lunk, J. Phys. D: Appl. Phys., 27 (2004) 3000.

41. I. P. Vinogradov and A. Lunk, Plasma Process. Polym., 2 (2005) 201.

42. R. d'Agostino, F. Cramarossa, F. Fracassi and F. Illuzzi, in R. d'Agostino (ed.), Plasma Deposition, Treatment and Etching of Polymers, Academic Press, New York, 1990, p. 95.

43. R. d'Agostino, in R. d'Agostino, P. Favia and F. Fracassi (Eds.), Plasma Processing of Polymers, NATO ASI Series, E: Applied Science, 346, Kluwer Academic Publishers, Dordrecht, 1997, p. 3.

44. F. Fanelli, F. Fracassi and R. d'Agostino, Plasma Process. Polym., 4 (2007) S430.

45. F. Fracassi, E. Occhiello and J.W. Coburn, J. Appl. Phys., 62 (1987) 3980.

46. G.S. Oehrlein and J.F. Rembetski, IBMJ Res. Develop., 36 (1992) 140.

47. F. Fanelli, Plasma Process. Polym., 5 (2009) 547.

48. M. Rokni, J. H. Jacob, J. A. Mangano and R. Brochu, Appl. Phys. Lett., 31 (1977) 79.

49. Ch. Brau, in Ch. K. Rhodes (ed.), Excimer Lasers, Topics in Applied Physics, Vol. 30, 2nd Ed., Springer-Verlag, Berlin Heidelberg, 1984, p. 87.

50. F. Fanelli, G. Di Renzo, F. Fracassi and R. d'Agostino, Plasma Process. Polim., 6 (2009) S503.

51. R. Chen, V. Gorelik and M. S. Silverstein, J. Appl. Polym. Sci., 56 (1995) 615.

52. A. M. Wrobel and M. Wertheimer, in R. d'Agostino (ed.), Plasma Deposition, Treatment, and Etching of Polymers, Academic Press, New York, 1990, p. 163.

53. A. M. Wrobel, A. Walkiewicz-Pietrzykowska, S. Wickramanayaka and Y. Hatanaka, J. Electrochem. Soc., 145 (1998) 2866.

54. M. Creatore, F. Palumbo and R. d'Agostino, Plasmas Polym., 7 (2002) 291.

55. G. Borvon, A. Goullet, A. Granier and G. Turban, Plasmas Polym., 7 (2002), 241.

56. F. Fracassi, R. d'Agostino, F. Fanelli, A. Fornelli and F. Palumbo, Plasmas Polym., 8 (2003).

57. Y. Sawada, S. Ogawa and M. Kogoma, J. Phys. D: Appl. Phys., 28 (1995) 1661.

58. A. Sonnenfeld, T. M. Tun, L. Zajıckova, K. V. Kozlov, H. E. Wagner, J. F. Behnke and R. Hippler, Plasmas Polym., 6 (2001) 237.

59. S. E. Alexandrov and, M. L. Hitchman, Chem. Vap. Deposition, 11 (2005) 457.

60. F. Massines, N. Gherardi, A. Fornelli and S. Martin, Surf. Coat. Technol., 200 (2005) 1855.

61. H. Caquineau, I. Enache, N. Gherardi, N. Naudé and F Massines, J. Phys. D: Appl. Phys., 42 (2009) 125201.

62. X. Zhu, F. Arefi-Khonsari, C. Petit-Etienne and M. Tatoulian, Plasma Processes Polym., 2 (2005) 407.

63. C. Petit-Etienne, M. Tatoulian, I. Mabille, E. Setter and F. Arefi- Khonsari, Plasma Processes Polym. 4 (2007) S562.

64. D. Vangeneugden, S. Paulussen, O. Goossens, R. Rego and K. Rose, Chem. Vap. Dep., 11 (2005) 491.

65. B. Twomey, M. Rahman, G. Byrne, A. Hynes, L.-A. O'Hare and L. O'Neill, D. Dowling, Plasma Processes Polym., 5 (2008) 737.

66. I. Vinogradov, D. Zimmer and A. Lunk, Plasma Processes Polym., 6 (2009) S514.

67. Fanelli, S. Lovascio, R. d'Agostino, F. Arefi-Khonsari and F. Fracassi, Plasma Process. Polym., (2010), DOI: 10.1002/ppap.200900159.

Figure captions

Fig. 1. Side-view of a parallel plate DBD fed by Ar-N_2 mixtures at various N_2 concentration (20 kHz, 4.8 kV_{p-p}, 2 mm discharge gap, 13.6 cm electrode width, 21 cm electrode length).

Fig. 2. (a) Side-view of a parallel plate FDBD fed by a Ar-0.6% CF_4 mixture, with a Si substrate; (b) crater onto the Si substrate surface (optical microscope image) exposed to the discharge (10 kHz, 7.6 kV_{p-p}, 2 mm discharge gap, 10 min treatment duration).

Fig. 3. Trend of the WCA of fluorocarbon thin films deposited in He-C_3F_8-H_2 GDBDs as a function of the CH-to-CF_2 emissions intensity ratio [29,44].

Fig. 4. Glass substrate coated with a fluoropolymer deposited in Ar-CF_4-20%H_2 FDBD. Etching-deposition competition in FDBD fed with Ar–CF_4–H_2 (a) and Ar–CF_4–O_2 (b) mixtures (O_2 and H_2 concentrations are calculated with respect to the total flow rate of reactive gas, CF_4–O_2 or CF_4–H_2) [32].

Fig. 5. Emission spectra of Ar-O_2-CF_4 fed FDBDs as a function of the [O_2] in the feed ([O_2] is considered with respect to the total flow rate of reactive gas, CF_4–O_2) [47].

Fig. 6. Deposition rate and XPS F/C ratio of fluorocarbon coatings deposited in FDBDs fed by Ar-0.2%C_3F_6 and increasing concentration of air and water vapour [50].

Fig. 7. FT-IR spectra of thin films deposited by FDBDs fed by Ar, O_2 and different methyldisiloxanes (i.e. HMDSO, PMDSO and TMDSO) at O_2-to-monomer ratios in the feed of 0 and 12.

Fig. 8. Monomer depletion evaluated through the GC-MS analysis of the exhaust gas of FDBDs fed by Ar, O_2 and different methyldisiloxanes (i.e. HMDSO, PMDSO and TMDSO), as a function of the O_2-to-monomer ratio in the feed.

Fig. 9. Hydroxypentamethyldisiloxane flow rate in the exhaust gas of FDBDs fed by Ar, O_2 and HMDSO or PMDSO as a function of the O_2-to-monomer ratio in the feed

Fig 1 colour

Click here to download high resolution image

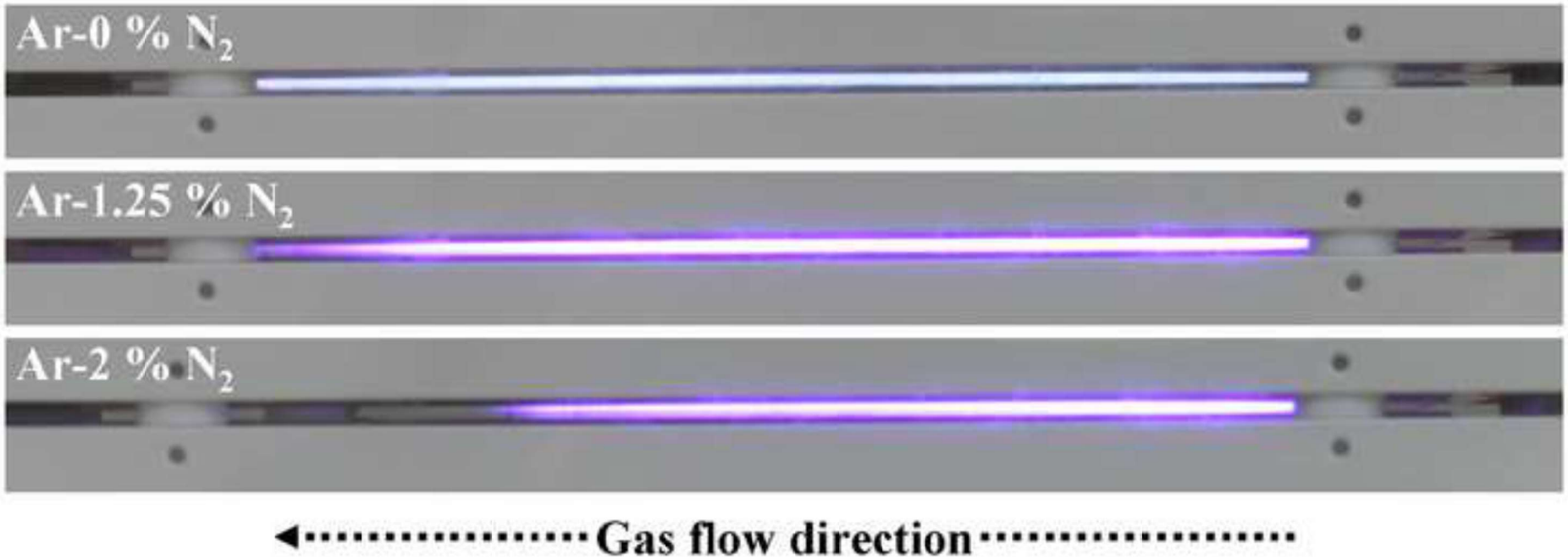

Fig 1 grey scale
Click here to download high resolution image

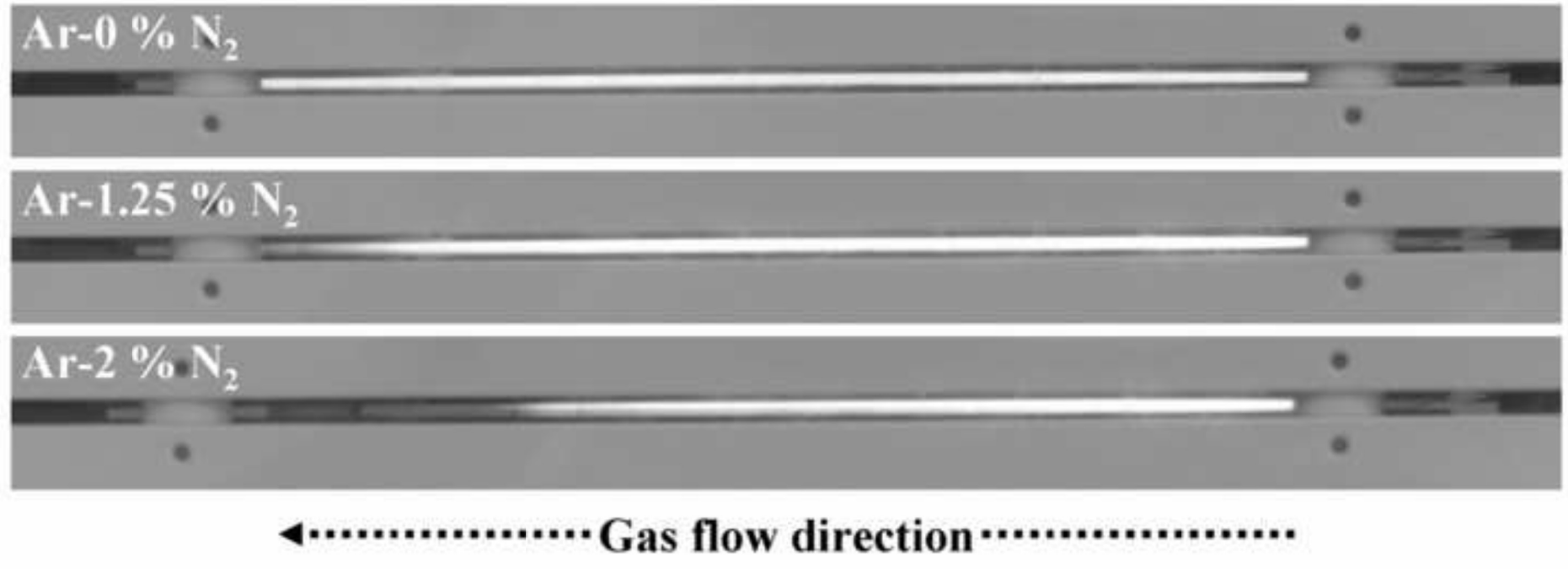

Fig 2 colour
Click here to download high resolution image

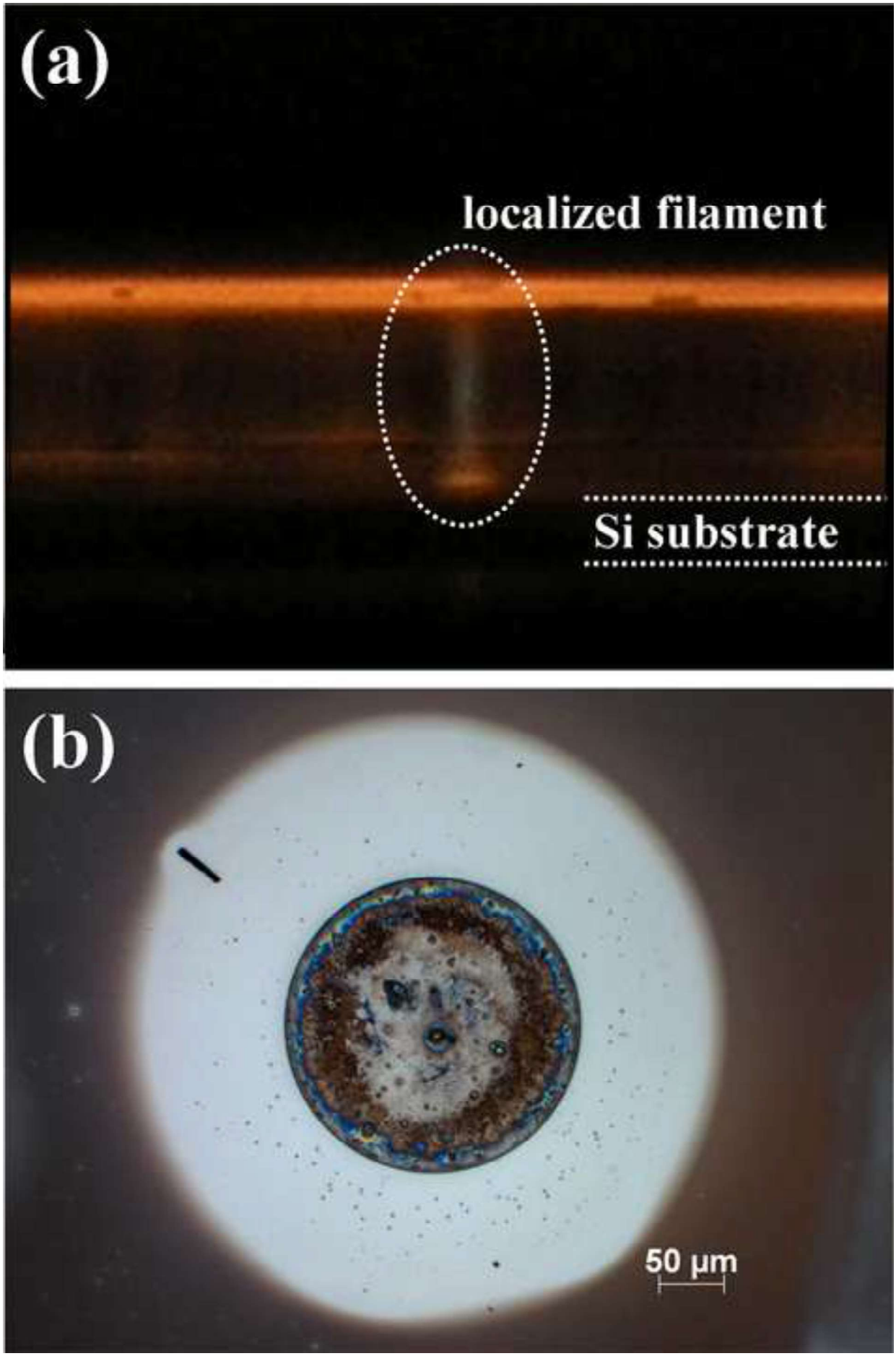

Fig 2 grey scale
Click here to download high resolution image

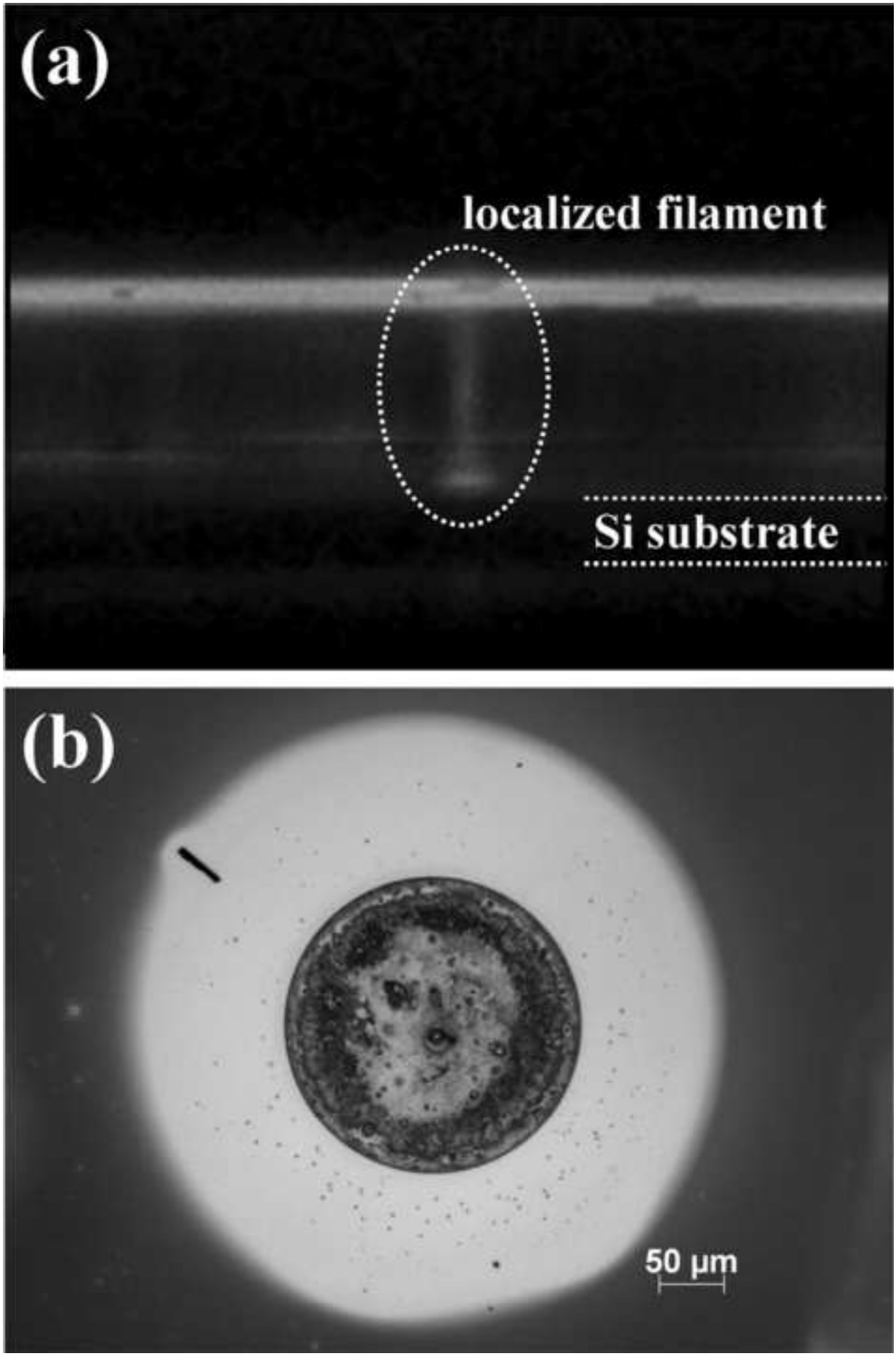

Fig 3
Click here to download high resolution image

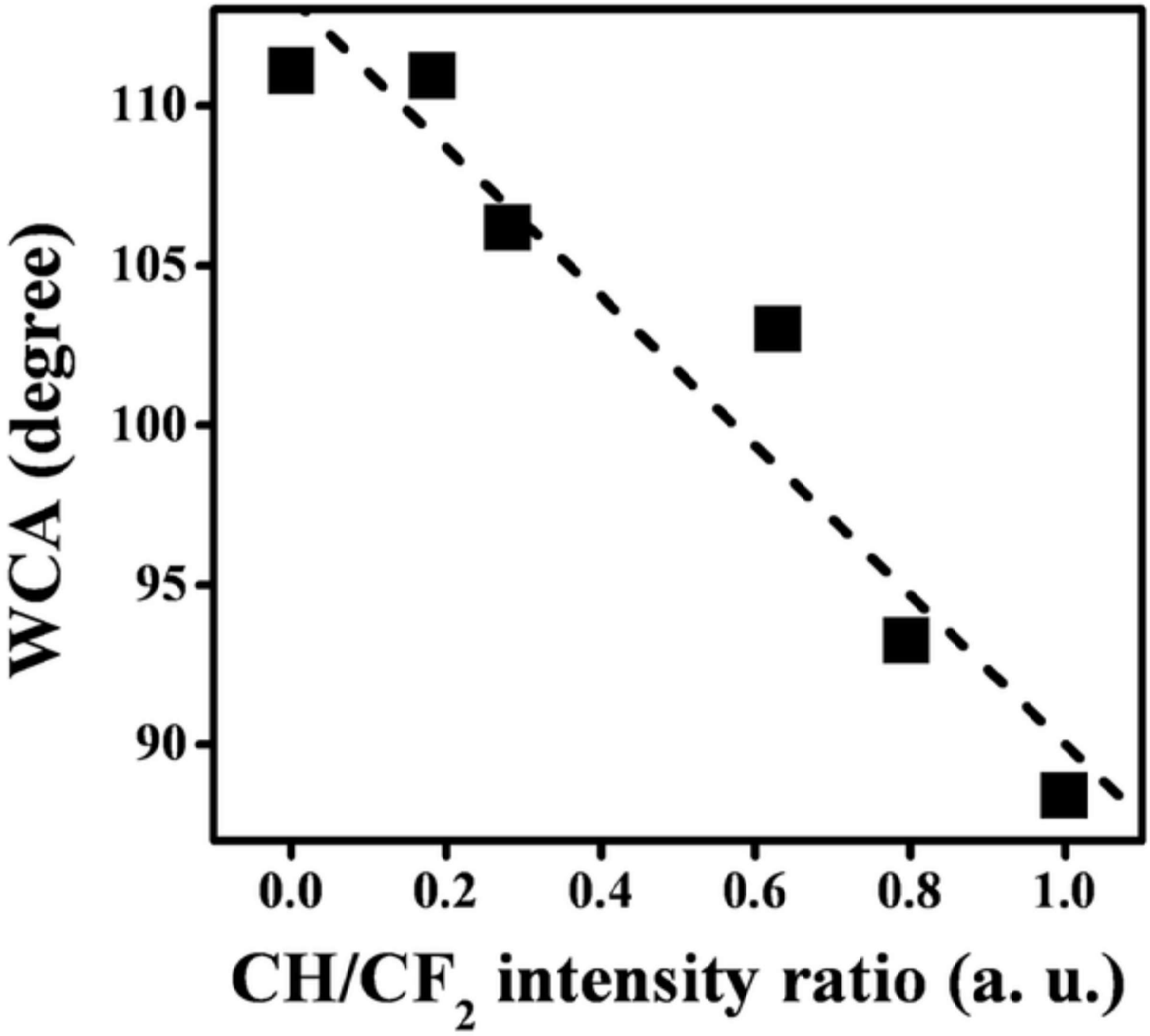

Fig 4
Click here to download high resolution image

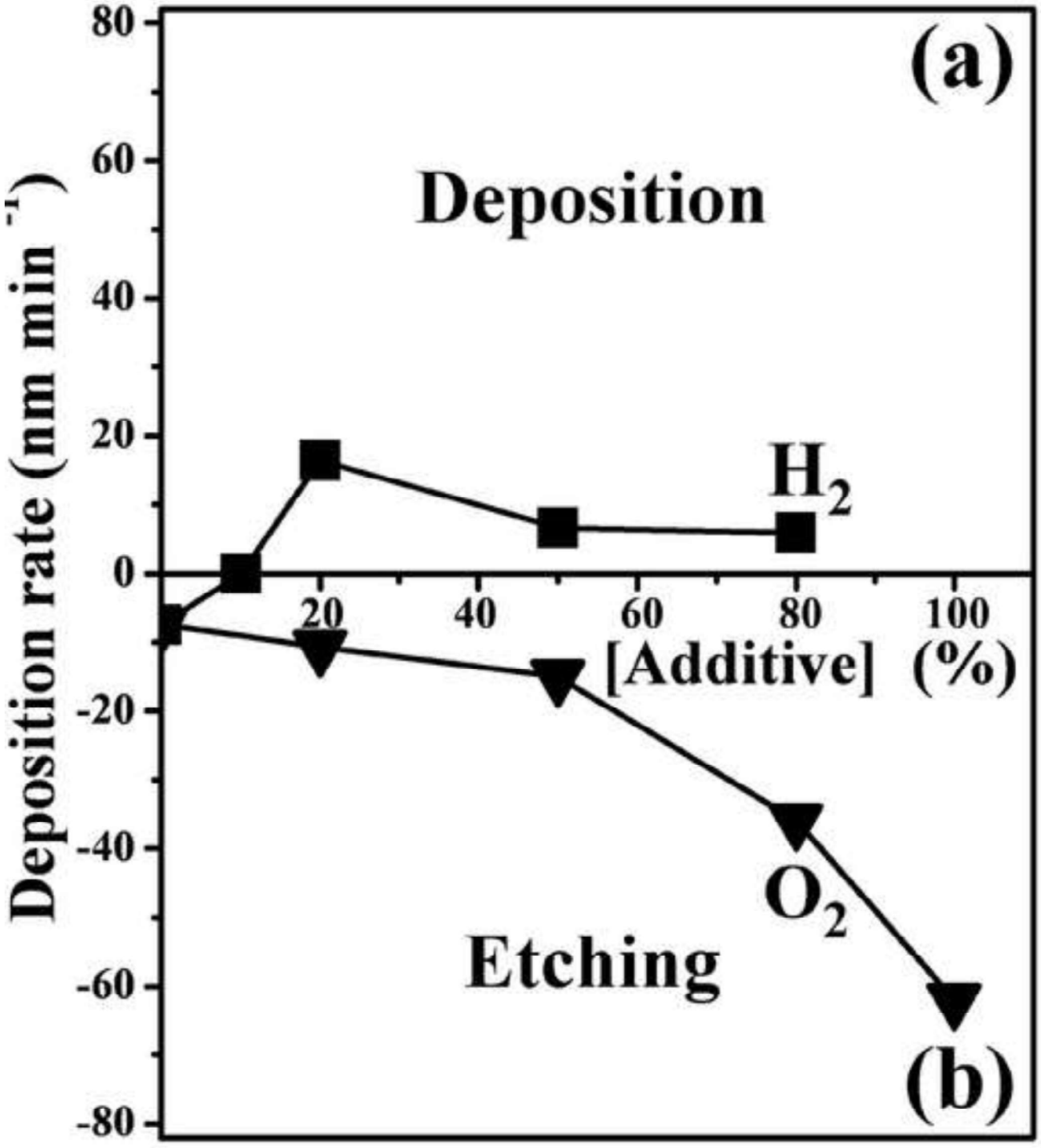

Fig 5
Click here to download high resolution image

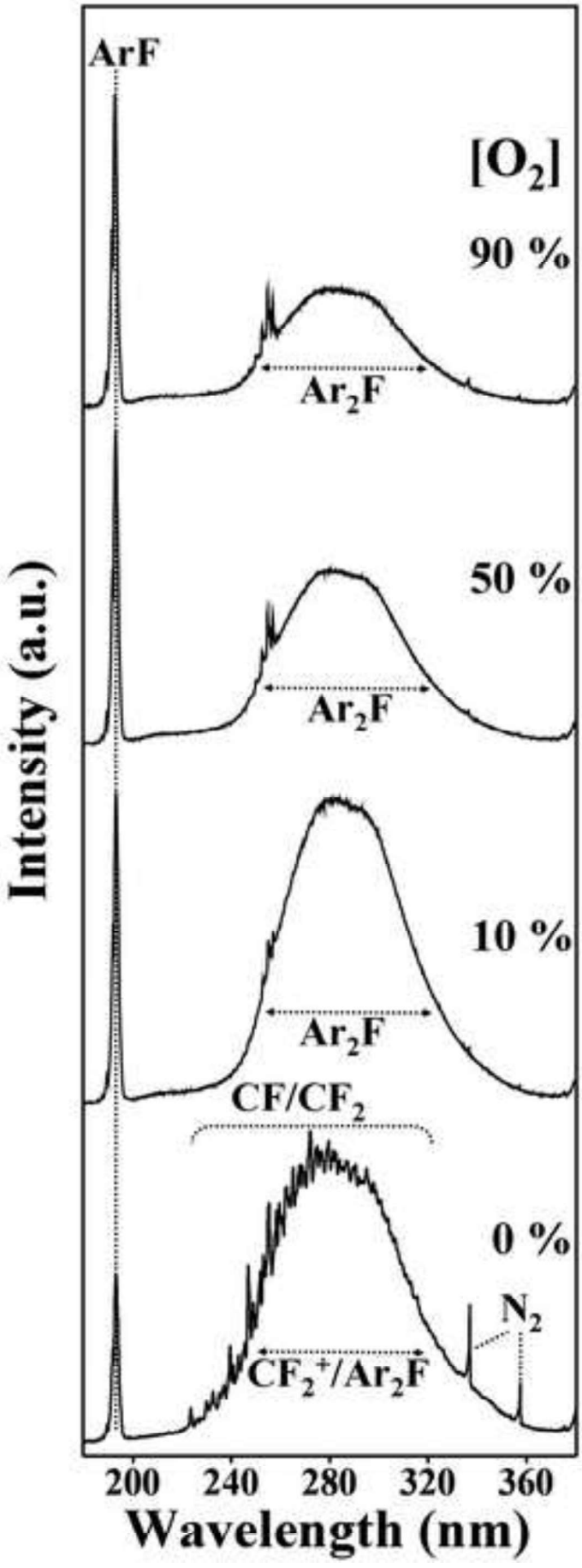

Fig 6
Click here to download high resolution image

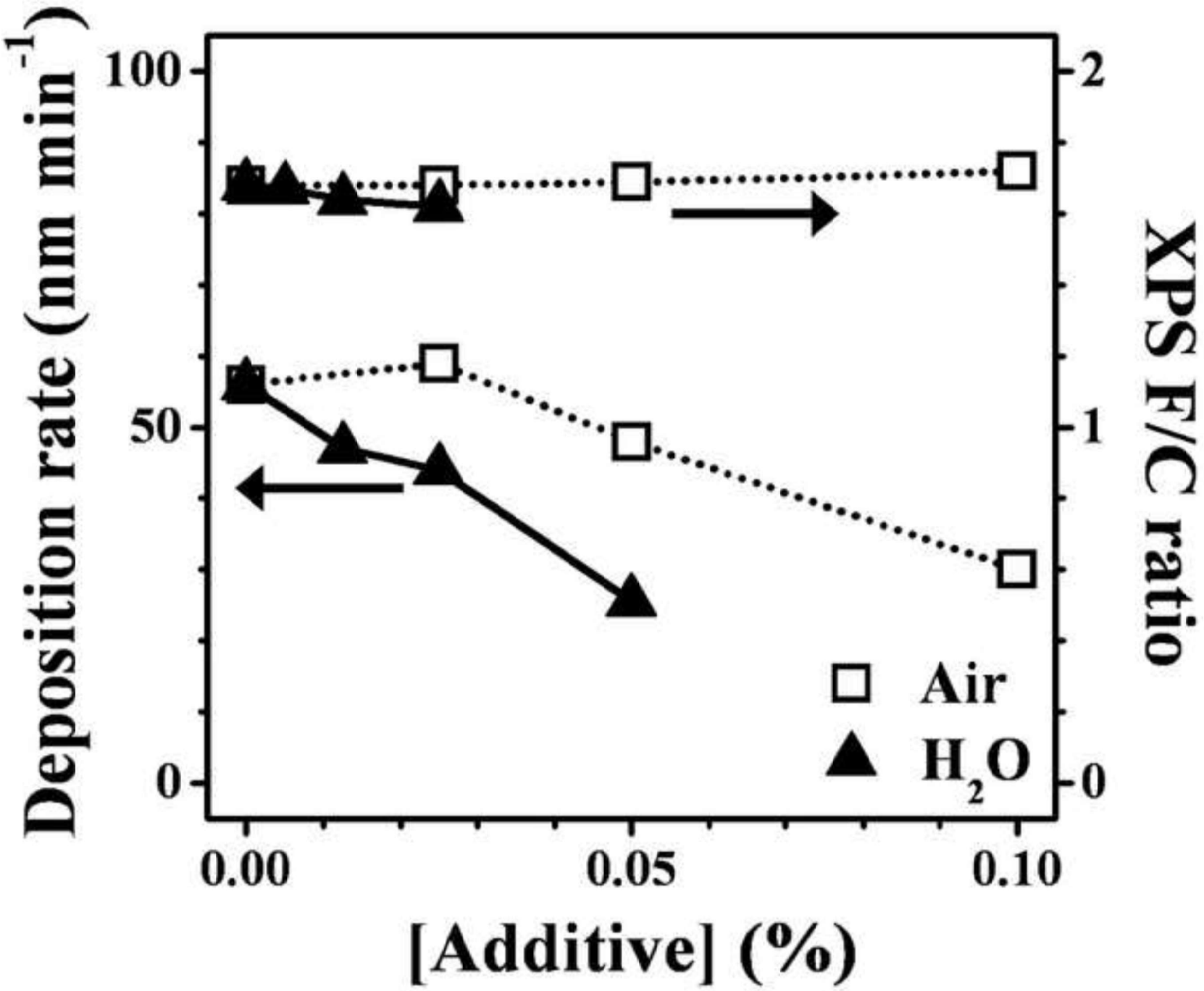

Fig 7
Click here to download high resolution image

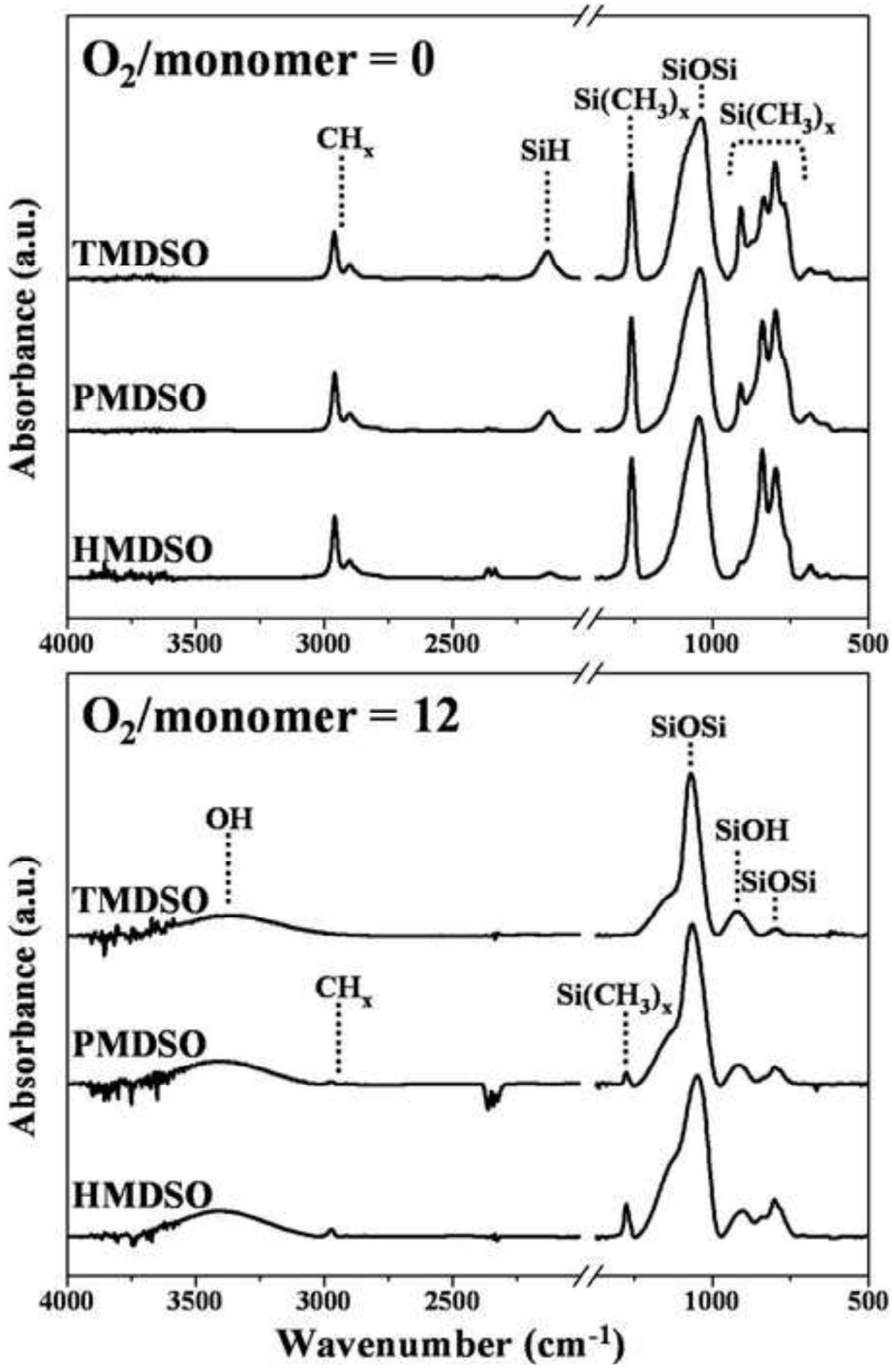

Fig 8
Click here to download high resolution image

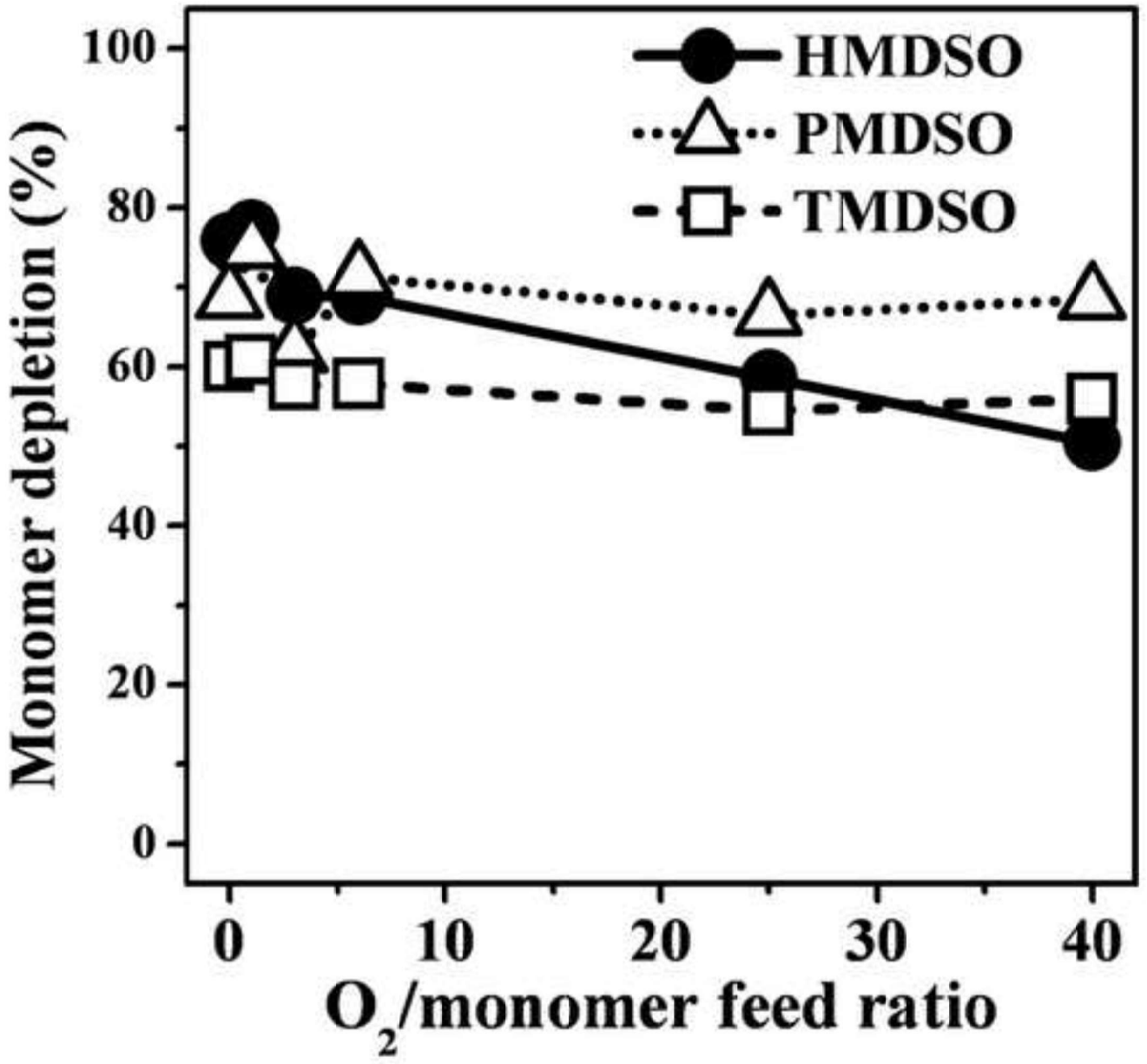

Fig 9
Click here to download high resolution image